

GLOBAL DOCUMENTATION OF GULLIES WITH THE MARS RECONNAISSANCE ORBITER CONTEXT CAMERA (CTX) AND IMPLICATIONS FOR THEIR FORMATION. T. N. Harrison^{1*}, G. R. Osinski^{1,2}, and L. L. Tornabene¹, ¹Centre for Planetary Science and Exploration/Department of Earth Sciences, University of Western Ontario, ²Department of Physics and Astronomy, University of Western Ontario. (*tanya.harrison@cpsx.uwo.ca)

Introduction: A number of models have been proposed to explain the formation of Martian gullies, including both “dry” [1,2] and “wet” mechanisms such as the release of liquid water/brine from shallow [3] or deep [4] aquifers or through the melting of near-surface ground ice [5] or snowpacks [6,7]. Previous surveys of gully distribution have been conducted to investigate their formation using either MOC narrow-angle (NA) images [8,9] (~1.4–12 m/pixel), or MOC NA images combined with Mars Odyssey Thermal Emission Imaging System visible subsystem data (THEMIS VIS, ~18 m/pixel) [10] and Mars Express High Resolution Stereo Camera (HRSC, 12.5–50 m/pixel) data [11,12]. However, surveys utilizing only MOC NA suffered from low spatial coverage (<1% of the planet) and sampling biases due to the narrow image footprint. While lower resolution datasets provided larger spatial coverage (~6% of the planet by Balme et al. [11] and ~42% by Kneissl et al. [12]), many gullies are not resolvable at THEMIS VIS and HRSC scale. Kneissl et al. [12] noted that ~42% of the gullies imaged with MOC NA in their survey could not be detected by HRSC due to their small size. Poor atmospheric conditions and unfavorable illumination angles were also cited as detection issues. CTX has covered ~85% of Mars at a resolution of ~6 m/pixel through the end of phase D09 (February 2013). CTX provides large aerial coverage at a resolution capable of resolving >95% of Martian gullies and removes any sampling bias from previous MOC NA studies [13]. Landforms potentially hosting gullies were specifically targeted by CTX during optimal illumination and atmospheric conditions to maximize detectability [13].

Methods: We inspected all 54,040 CTX images acquired during phases T01–D09 planet-wide to search for occurrences of gullies, documenting their setting, the geographic coordinates of each gullied landform, and their orientation. We follow the definition of Malin and Edgett [3], who defined gullies as consisting of three characteristic features: Alcove, channel, and apron. Features in the equatorial regions classified as gullies by some authors [1,2] lack the incised channels of mid- to high-latitude gullies, which often display fluvial characteristics such as tributaries, streamlined features, and terraces [14]. Therefore, these features are not considered gullies in this study.

Results: We have documented 4861 separate gullied landforms (e.g., individual craters, massifs, valleys, etc.), hosting tens of thousands of individual gullies (Fig. 1). This data confirms that gullies are confined to ~27–83°S and ~28–72°N and span all longitudes (roughly consistent with previous surveys [8–12]) and span all longitudes. A notable difference in this survey compared to all previous gully surveys is the observation of gullies on the floors of the Hellas and Argyre basins. Regional clustering is observed in both hemispheres, as well as regions lacking gullies. In general, northern hemisphere gullies tend to be much less developed and more heavily eroded than their southern counterparts, and pole-facing gullies tend to be more developed than equator-facing gullies in both hemispheres.

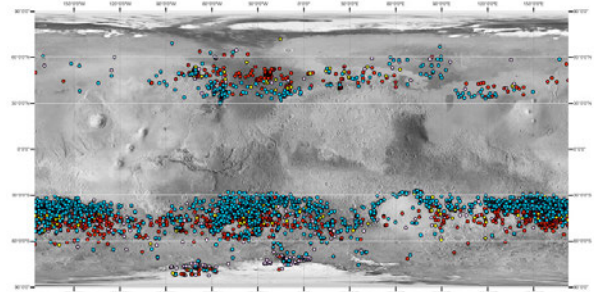


Fig. 1. Global distribution of gullied landforms. White lines indicate 30° and 60° N/S latitude. Colors indicate dominant gully orientation at each landform; blue = pole-facing, yellow = east-west facing, red = equator-facing, and purple = no preference.

A clear transition in dominant gully orientation is observed in the southern hemisphere, moving from poleward-facing preference in the lower mid-latitudes to equator-facing at ~45°S. The transition of pole-facing to equator-facing preference with increasing latitude is also roughly observed in the northern hemisphere, most clearly in Acidalia, at ~40°N. Poleward of 50°N, no dominant orientation preference is observed. These observations in both hemispheres are broadly consistent with previous studies utilizing less areally extensive coverage [8–12].

Implications: Figure 2 shows the locations of gullies relative to areas of ice accumulation at 35° obliquity as predicted by the modeling of Madeleine et al. [15]. In both hemispheres, the clusters of gullies are roughly anti-correlated with the areas of maximum ice accumulation; 75% of gullied landforms lie outside

these areas in the southern hemisphere, while 42% occur outside in the north. No correlation is observed between gullies and the present-day distribution of near-surface ground ice [e.g., 16, 17].

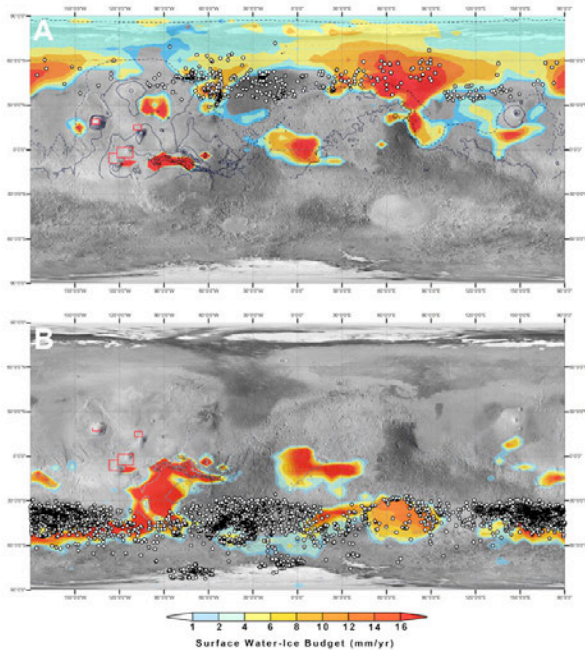


Fig 2. Locations of gullies plotted atop ice accumulation model results from Madeleine et al. [16]. Ice accumulation shown for model results at $\epsilon = 35^\circ$, $e = 0.1$, $\tau_{\text{dust}} = 2.5$, and (a) longitude of perihelion $L_p = 270^\circ$ and (b) $L_p = 90^\circ$.

Based on these observations, we suggest that the latitudinal distribution, shift in orientation preference with increasing latitude, and location relative to areas of predicted ice accumulation at higher obliquity all point towards insolation and atmospheric conditions playing key roles in gully formation. Combining these observations with the models of Madeleine et al. [15] and Christensen [6], we propose the following sequence of events:

1. At high ($\sim 45^\circ$) obliquity, ice is transported from the poles to the tropics [18].
2. As obliquity shifts to more moderate values ($\sim 35^\circ$), ice is transported from the tropics to the mid- and high-latitudes [15].
3. Storm activity driven by temperature gradients at the margins of the mid-latitude ice sheets results in the precipitation of snow in winter, which is concentrated onto slopes and in topographic hollows (such as alcoves in eroding crater walls) by wind. This process facilitates the accumulation of localized snowpacks significantly thicker than the annual average precipitation [e.g., 19].
4. In spring and summer, increased dust storm activity results in the accumulation of dust

atop the snowpacks, helping to preserve the underlying snow. In favorable locations, melting occurs via solar insolation, resulting in erosion to slowly form gullies over extended periods of time [e.g., 6, 7].

5. As obliquity shifts to lower values ($\sim 25^\circ$), the mid-latitude ice sheets begin to retreat, resulting in storm activity (and hence snow and dust accumulation) over previously ice-covered areas. Gully erosion continues in the mid-latitudes and begins in the higher latitudes, slowing as atmospheric and insolation conditions approach those of present-day Mars.

This sequence of events explains the global distribution of gullies, the greater maturity of mid- vs. high-latitude gullies, and the greater general evolution of pole-facing vs. equator-facing gullies: snowpacks should be better preserved on pole-facing slopes [6], providing a source of meltwater for longer periods. It is important to note that while the global distribution of gullies suggests a common control on their formation, not all of their discrete formation mechanisms are necessarily the same. As present-day gully activity has been documented [e.g., 13, 20, 21], liquid water may still persist at some periods in these areas, possibly providing a habitable environment and therefore making these locations significant astrobiological targets for investigation.

References: [1] Treiman A. H. (2003) *JGR*, 108, 8031. [2] Shinbrot T. et al. (2004) *PNAS*, 101, 8542–8546. [3] Malin M. C. and Edgett K. S. (2000) *Science*, 288, 2330–2335. [4] Gaidos E. J. (2001) *Icarus*, 153, 218–223. [5] Costard F. et al. (2002) *Science*, 295, 110–113. [6] Christensen P. R. (2003) *Nature*, 422, 45–48. [7] Williams K. E. et al. (2008) *Icarus*, 196, 565–577. [8] Heldmann J. L. and Mellon M. T. (2004) *Icarus*, 168, 285–304. [9] Heldmann J. L. et al. (2007) *Icarus*, 188, 324–344. [10] Bridges N. T. and Lackner C. N. (2006) *JGR*, 111, E09014. [11] Balme M. et al. (2006) *JGR*, 111, E05001. [12] Kneissl T. et al. (2010) *EPSL*, 294, 357–367. [13] Harrison T. N. et al. (2009) *BAAS*, 41, 1113. [14] McEwen A. S. et al. (2007) *JGR*, 112, E05S02. [15] Madeleine J. –B. et al. (2009) *Icarus*, 203, 390–405. [16] Boynton W. V. et al. (2002) *Science*, 297, 81–85. [17] Plaut J. J. et al. (2009) *LPSC 40*, abstract #2312. [18] Levrard B. et al. (2004) *Nature*, 431, 1072–1075. [19] Dickson J. L. and Head J. W. (2009) *Icarus*, 204, 63–86. [20] Malin M. C. et al. (2006) *Science*, 314, 1573–1577. [21] Dundas C. M. et al. *GRL*, 37, L07202.

Acknowledgements: This work was partially funded by the NSERC CREATE Technologies and Techniques for Space Exploration and Canadian Astrobiology Training Program Ph.D. fellowship programs.